

## Charge delocalization and structural response in layered $\text{La}_{1.2}\text{Sr}_{1.8}\text{Mn}_2\text{O}_7$ : Enhanced distortion in the metallic regime

J. F. Mitchell

*Materials Science Division, Argonne National Laboratory, Argonne, Illinois 60439*

D. N. Argyriou

*Science and Technology Center for Superconductivity, Argonne National Laboratory, Argonne, Illinois 60439*

J. D. Jorgensen, D. G. Hinks, C. D. Potter, and S. D. Bader

*Materials Science Division, Argonne National Laboratory, Argonne, Illinois 60439*

(Received 17 September 1996)

Temperature-dependent neutron diffraction studies on melt-grown crystals of the layered compound  $\text{La}_{1.2}\text{Sr}_{1.8}\text{Mn}_2\text{O}_7$  reveal a dramatic structural response to the onset of ferromagnetism and the coincident insulator-metal transition. Unlike the related manganite perovskites, whose Jahn-Teller distorted octahedra become more regular at temperatures below the insulator-metal transition, the  $\text{MnO}_6$  octahedra of this layered material are more severely distorted when the charge is itinerant than when it is localized.

[S0163-1829(97)04701-2]

Current research in the mixed valent manganite perovskite materials has expanded to include the search for materials with other structure types exhibiting “colossal” magnetoresistance (CMR). Shimakawa *et al.*<sup>1</sup> have reported CMR in a pyrochlore ( $\text{Ti}_2\text{Mn}_2\text{O}_7$ ) synthesized at high pressure, and Cheong *et al.* have studied In substitution in this system.<sup>2</sup> Moritomo *et al.* have recently published a single crystal study of layered  $\text{La}_{1.2}\text{Sr}_{1.8}\text{Mn}_2\text{O}_7$ ,<sup>3</sup> the  $n=2$  member of the Ruddlesden-Popper series  $(\text{La,Sr})_{n+1}\text{Mn}_n\text{O}_{3n+1}$ . They found a  $\sim 20\,000\%$  MR (129 K,  $H=7$  T) in this layered material and speculated on the role of reduced dimensionality in the electronic transport. This material may also be important due to its pronounced CMR in low field,  $\sim 200\%$  at 129 K in 0.3 T.

We have grown crystals of  $\text{La}_{1.2}\text{Sr}_{1.8}\text{Mn}_2\text{O}_7$  and collected temperature dependent neutron powder diffraction data to study the structural response of this two-dimensional CMR material at the magnetic and electronic phase transitions. Like the three-dimensional perovskites,  $\text{La}_{1.2}\text{Sr}_{1.8}\text{Mn}_2\text{O}_7$  exhibits a dramatic structural response to the onset of ferromagnetism and the coincident delocalization of charge. However, unlike the three-dimensional perovskite systems, whose Jahn-Teller distorted octahedra become more regular for temperatures below the insulator-metal transition, this layered  $\text{La}_{1.2}\text{Sr}_{1.8}\text{Mn}_2\text{O}_7$  exhibits an enhanced distortion of the  $\text{MnO}_6$  octahedron in the metallic regime. The nature of this enhanced distortion—a “one-long, five-short”  $\text{MnO}_6$  octahedron—provides further information concerning the geometric parameters important to localized and itinerant electronic states in the manganite family.

Crystals of  $\text{La}_{1.2}\text{Sr}_{1.8}\text{Mn}_2\text{O}_7$  were melt-grown in flowing 20%  $\text{O}_2$  (balance Ar) using a floating zone optical image furnace (NEC Model SC-M15HD). The resulting boule is polycrystalline and cleaves readily to yield shiny black crystals. Energy dispersive spectroscopy (Oxford Instruments Link Isis) indicates that the metal stoichiometry is equal to the nominal composition within experimental error. A 2.8 g

sample was cut from the as-grown boule in a region near to the terminus of the crystal growth. A small piece of this sample was used for measurement of four-lead resistance and ac susceptibility (Lakeshore Cryotronics Model 7000 ac susceptometer). The remainder of the sample was thoroughly pulverized for neutron powder diffraction experiments.

Time-of-flight neutron powder diffraction patterns were measured using the Special Environment Powder Diffractometer<sup>4</sup> (SEPD) at Argonne National Laboratory’s Intense Pulsed Neutron Source. Data were collected from 20–300 K on a Displex refrigerator and from 300–508 K in a radiation furnace. The sample was contained in a sealed vanadium can with He exchange gas in both cases. Data were analyzed using the program GSAS.<sup>5</sup> For patterns collected below 120 K, a magnetic moment on the Mn site was refined. No intensity attributable to magnetic scattering was observed for  $T > 120$  K. Refinement of the  $\text{La}_{1.2}\text{Sr}_{1.8}\text{Mn}_2\text{O}_7$  phase was carried out in space group  $I4/mmm$  for all temperatures. A second phase identified as  $(\text{La,Sr})_2\text{MnO}_4$  (Refs. 6 and 7) was included in the refinements, which showed that

TABLE I. Structural parameters determined from Rietveld analysis of neutron powder diffraction data collected at 404 K. For refinements at all temperatures the space group  $I4/mmm$  was used. For this temperature the measured lattice parameters are  $a=3.87424(2)$  Å and  $c=20.1454(2)$  Å. The agreement indices for this refinement are  $R_{wp}=3.98\%$  and  $R(F^2)=5.99\%$ .

Atom	x	y	z	$B$ (Å <sup>2</sup> )	Occupancy
La,Sr(1) <sup>a</sup>	0	0	0.5	0.60(2)	1.01(1)
La,Sr(2) <sup>a</sup>	0	0	0.317 49(6)	0.6(2)	1.01(1)
Mn	0	0	0.096 4(1)	0.26(3)	1.0 <sup>b</sup>
O(1)	0	0	0	1.30(6)	1.05(2)
O(2)	0	0	0.195 87(9)	1.1(4)	0.97(1)
O(3)	0	0.5	0.095 15(5)	0.99(2)	1.07(1)

<sup>a</sup> $B[\text{La,Sr}(1)]=B[\text{La,Sr}(2)]$ ; occupancy  $[\text{La,Sr}(1)]=\text{occupancy}[\text{La,Sr}(2)]$ .

<sup>b</sup>Occupancy of the Mn site was not refined.

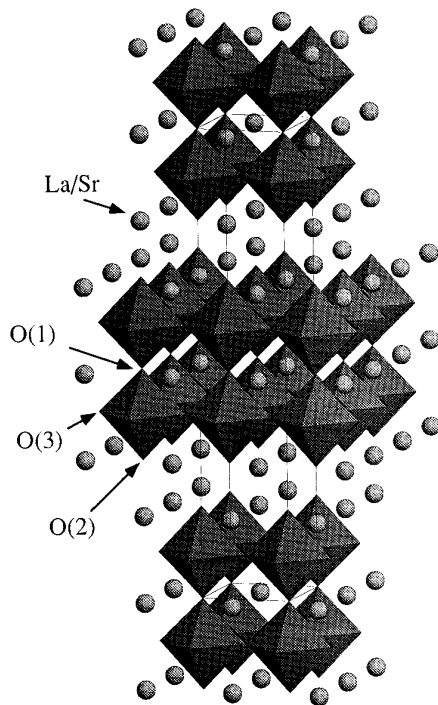


FIG. 1. Crystal structure of  $\text{La}_{1.2}\text{Sr}_{1.8}\text{Mn}_2\text{O}_7$ . The  $\text{MnO}_6$  octahedra are shaded. The (La,Sr) site is shown as a sphere.

this phase accounts for  $\sim 10\%$  of the sample by mass. This phase was found in samples examined from throughout the boule. Results of the Rietveld refinement for data collected at 404 K (in the paramagnetic regime) are presented in Table I. Refinement of occupancies indicates that all sites are fully occupied, with the possible exception of the apical oxygen site, O(2), which may be slightly deficient. Figure 1 shows the structure of layered  $\text{La}_{1.2}\text{Sr}_{1.8}\text{Mn}_2\text{O}_7$ .

Figure 2 shows the magnetic and transport behavior of  $\text{La}_{1.2}\text{Sr}_{1.8}\text{Mn}_2\text{O}_7$  as a function of temperature. A sharp transition is observed in both measurements at 120 K, signaling the onset of ferromagnetic order and an associated insulator-metal transition. These coincident magnetic and electronic transitions are common in perovskite CMR materials and have been observed both by Moritomo *et al.*<sup>3</sup> in their single crystal study of  $\text{La}_{1.2}\text{Sr}_{1.8}\text{Mn}_2\text{O}_7$  and by Mahesh *et al.* in polycrystalline samples of  $\text{La}_{1.4}\text{Sr}_{1.6}\text{Mn}_2\text{O}_7$ .<sup>7</sup> In the range 270–300 K there is an additional feature found in the ac susceptibility. This feature does not originate from the impurity phase since the single layer  $(\text{La,Sr})_2\text{MnO}_4$  compounds are paramagnetic for  $T > 150$  K.<sup>6,7</sup> MacChesney *et al.*<sup>8</sup> observed a similar “terraced” behavior in magnetization data from polycrystalline samples of  $\text{La}_{1.33}\text{Sr}_{1.66}\text{Mn}_2\text{O}_7$ ,<sup>12</sup> and speculated that spin correlations above  $T_C$  might be intrinsic to this class of two-dimensional materials. Moritomo *et al.* likewise claim that two-dimensional spin correlation is responsible for the moment they observe in  $\text{La}_{1.2}\text{Sr}_{1.8}\text{Mn}_2\text{O}_7$  single crystals at temperatures above  $T_C$ . Since our neutron diffraction patterns reveal no evidence of magnetic scattering for  $T > 120$  K, any such magnetic correlations are on a short-range length scale relative to that of the neutron diffraction experiment.

Figure 3 shows the temperature evolution of the unit cell volume and the tetragonal lattice parameters. Like

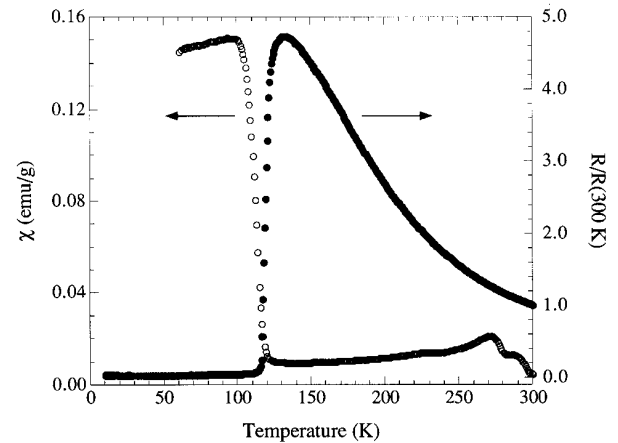


FIG. 2. ac susceptibility ( $H=0.1$  Oe; 100 Hz) and resistance (normalized to  $R_{300\text{ K}}$ ) vs temperature for  $\text{La}_{1.2}\text{Sr}_{1.8}\text{Mn}_2\text{O}_7$ .

the perovskite-based CMR materials,<sup>9–12</sup> layered  $\text{La}_{1.2}\text{Sr}_{1.8}\text{Mn}_2\text{O}_7$  shows dramatic lattice effects at  $T_C=120$  K. While these lattice effects occur over a narrow temperature range, our data suggest a continuous phase transition. The unit cell volume decreases monotonically with decreasing temperature with a change in slope at  $T_C$ . The volume decreases by  $\sim 0.1\%$  through the transition. A similar result has been reported for the perovskite  $\text{La}_{0.75}\text{Ca}_{0.25}\text{MnO}_3$  by Radaelli *et al.*<sup>12</sup> Similar to the perovskites, the unit cell axes change over a narrow temperature range near  $T_C$ ; the  $c$  axis expands by  $\sim 0.06\%$ , and the  $a$  axis contracts by  $\sim 0.16\%$ . However, for  $T > T_C$ , the  $a$  axis behaves quite differently than the  $c$  axis. Between 500 and 120 K the  $c$  axis contracts linearly with temperature, decreasing by 0.71%. From 500 to 300 K, the  $a$  axis contracts linearly with decreasing temperature by  $\sim 0.14\%$ . However, at  $T \sim 280$ –300 K, the thermal expansion of the  $a$  axis begins to deviate from linearity. Between 280 K and  $T_C$ , the  $a$  axis shrinks only an additional 0.03% before rapidly contracting beginning at  $T_C$ . As mentioned earlier, Moritomo *et al.* conclude from magnetization data that a finite moment exists above  $T_C$  in the form of two-dimensional spin correlations.<sup>3</sup> It is possible that the magnetic feature observed near room temperature in the ac susceptibility and the  $a$ -axis thermal expansion are coupled. Another possibility follows a suggestion by Ibarra *et al.*,<sup>11</sup> who have observed a similar deviation from linearity in the thermal expansion of polycrystalline  $\text{La}_{0.60}\text{Y}_{0.07}\text{Ca}_{0.33}\text{MnO}_3$  well above its Curie temperature. They attribute the effect to a gradual carrier localization process, a polaron effect. Our measurements do not allow us to distinguish between this suggestion or a spin-lattice coupling. Nonetheless, we can reasonably conclude from the absence of nonlinearity in the  $c$  axis thermal expansion near room temperature that the carrier localization or spin-lattice coupling occurs parallel to the perovskite layers and not perpendicular to them.

The temperature evolution of the three symmetry-independent Mn-O bond lengths suggests that the relationship between the Jahn-Teller distortion and electronic transport in the layered materials may be quite different than that observed in the perovskites. Caignaert *et al.*<sup>9</sup> have recently shown that the Jahn-Teller distortion coordinate  $D = d_{\text{Mn-O(apical)}}/d_{\text{Mn-O(equatorial)}}$  in  $\text{Pr}_{0.7}\text{Ca}_{0.25}\text{Sr}_{0.1}\text{MnO}_3$  increases with decreasing temperature and then dramatically

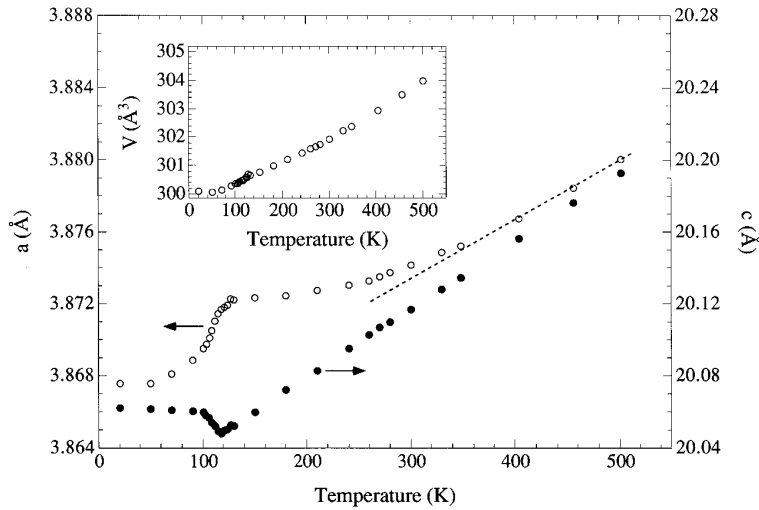


FIG. 3.  $\text{La}_{1.2}\text{Sr}_{1.8}\text{Mn}_2\text{O}_7$  lattice parameters vs. temperature. Error bars are smaller than the symbols. The dashed line is a guide to the eye. Inset: Unit cell volume vs temperature.

plummets at the metal-insulator transition. Such behavior indicates that in the perovskite the itinerant electron state is characterized by a less distorted  $\text{MnO}_6$  octahedron than the localized state. Radaelli *et al.* have reported a similar effect in  $\text{La}_{0.35}\text{Pr}_{0.35}\text{Ca}_{0.3}\text{MnO}_3$ .<sup>13</sup> Figure 4 shows the evolution of  $D$  with temperature in the two-dimensional  $\text{La}_{1.2}\text{Sr}_{1.8}\text{Mn}_2\text{O}_7$ . Here we have taken the average of  $\text{Mn-O}(1)$  and  $\text{Mn-O}(2)$  for  $d_{\text{Mn-O}(\text{apical})}$ . In contrast to the perovskites mentioned above,  $D$  slowly decreases with decreasing temperature until the onset of ferromagnetism at 120 K—and its attendant metal-insulator transition—where  $D$  sharply *increases* by  $\sim 0.6\%$ . Thus the delocalization of charge is accompanied by an increase in the distortion of the  $\text{MnO}_6$  octahedron, a distinct contrast with the perovskites.

Figure 5 and Table II give a more detailed picture of the Mn-O bond lengths as a function of temperature. In particular, they show that the equatorial Mn-O(3) bond tracks the  $a$  axis, contracting at the insulator-to-metal transition by  $\sim 0.14\%$ . Archibald and Goodenough<sup>14,15</sup> have suggested that such a contraction results from the localized Mn-O antibonding  $e_g$  electron becoming itinerant; the loss of antibonding electron density in the Mn-O bond results in its contraction. The apical bond to the oxygen lying between the two  $\text{MnO}_2$  layers, Mn-O(1), is only weakly temperature de-

pendent. In fact, five bonds (four equatorial, one apical) are quite similar for all temperatures measured and are essentially identical at 20 K (see Table II). It is the apical Mn-O(2) bond with its unshared oxygen atom that is longer than the other five bonds at all temperatures and that expands even more through the magnetic transition. The apical Mn-O(2) bond reaches a minimum at  $T_C$  and then increases from 1.984(4) to 2.002(4) Å (0.91%) at temperatures immediately below  $T_C$ . The increased Mn-O(2) bond may be a response of the system to the magnetic ordering, reflecting a charge transfer between the in-plane and apical Mn-O bonds. We have seen similar large Mn-O bond length effects in the ferromagnetic insulator  $\text{La}_{0.875}\text{Sr}_{0.125}\text{MnO}_3$ , where the charge remains localized through the ferromagnetic transition.<sup>10</sup>

We have suggested that in the perovskite manganites a

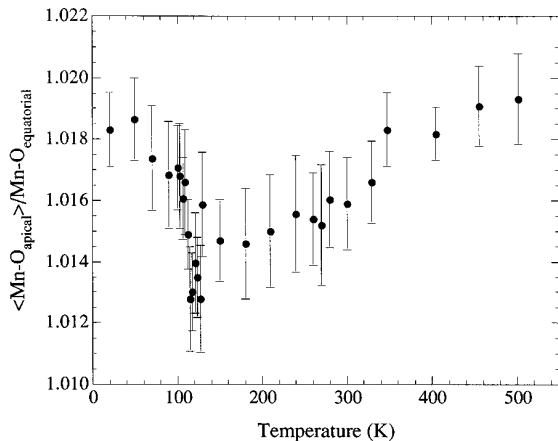


FIG. 4. Octahedral distortion,  $D = \langle \text{Mn-O}_{\text{apical}} \rangle / \text{Mn-O}_{\text{equatorial}}$ , vs temperature for  $\text{La}_{1.2}\text{Sr}_{1.8}\text{Mn}_2\text{O}_7$ .

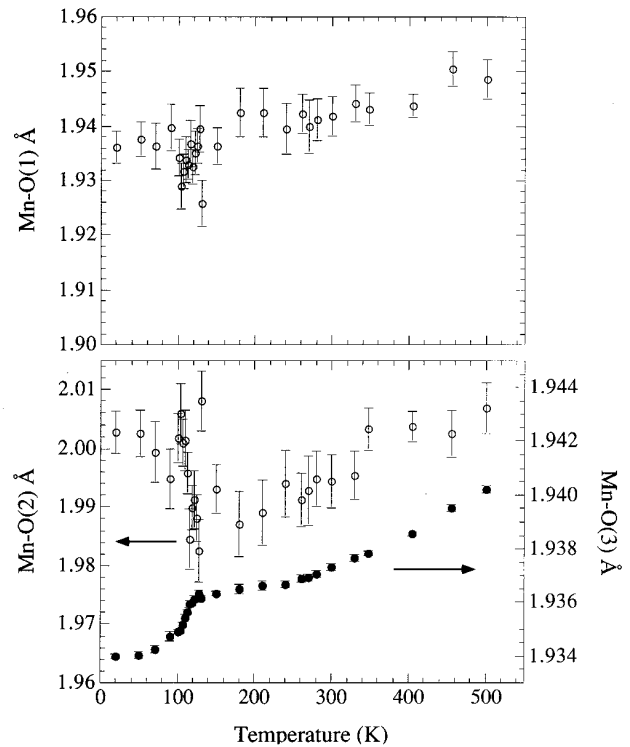


FIG. 5. Mn-O bond lengths vs temperature.

TABLE II. Selected bond lengths (Å) and angles (°) at various temperatures.

	20 K	180 K	300 K	404 K
Mn-O(1) Å	1.936(3)	1.942(4)	1.942(4)	1.944(2)
Mn-O(2) Å	2.003(4)	1.987(6)	1.994(5)	2.004(3)
Mn-O(3) Å	1.933 98(5)	1.9365(1)	1.937 33(7)	1.938 56(4)
Mn-O(3)-Mn	178.4(2)	178.1(3)	178.2(3)	178.5(2)
O(2)-Mn-O(3)	90.8(1)	90.9(1)	90.9(1)	90.8(1)

sufficiently large Jahn-Teller distortion prevents electron delocalization even in the ferromagnetic state.<sup>16</sup> Apparently, with its “one-long, five-short” geometry, the MnO<sub>6</sub> octahedra of the double layer are sufficiently regular to support a metallic state. It is possible that the double layer structure imposes a stereochemical constraint on the distortion coordinate, enforcing this degree of regularity. No temperature dependent structural data on the  $n=1$  member of this Ruddlesden-Popper series, La<sub>0.8</sub>Sr<sub>1.4</sub>MnO<sub>4</sub>, have been reported, but a fully developed Jahn-Teller distortion, i.e., both apical bonds highly distorted, in this compound would be consistent with its observed insulating behavior for  $T < 300$  K.<sup>3</sup>

At 404 K, the O(1)-Mn-O(2) angle and the O(2)-Mn-O(3) angle are 180° (by symmetry) and ~91°, respectively. As shown in Table II, O(2)-Mn-O(3) does not vary appreciably with temperature, showing that the octahedra distort only along a bond-stretching coordinate. Furthermore, the in-plane Mn-O(3)-Mn angle of ~178° at 404 K exhibits far less deviation from linearity than is typically found in the perovskite manganites (~160°),<sup>10,12,13,16–18</sup> this “buckling” angle is also insensitive to temperature. Such a small bending of the Mn-O-Mn angle implies a substantial one-electron bandwidth parallel to the layers.

For temperatures below 120 K the neutron diffraction patterns show intensity attributable to long-range ferromagnetic ordering of Mn spins. Rietveld refinement of the magnetic structure reveals that the Mn spins lie entirely within the  $a$ - $b$  plane. That is, this two-dimensional system exhibits no

spin canting along the  $c$  axis such as that observed in the three-dimensional (La,Sr)MnO<sub>3</sub> perovskite system.<sup>10</sup> Unfortunately, our data do not allow us to determine the direction of the Mn moment in the plane. The saturation moment obtained from our Rietveld refinement is 3.0(1)  $\mu_B$ /Mn at 20 K. This refinement is consistent with Moritomo’s magnetization data showing the easy axis lying in the MnO<sub>2</sub> plane and a ~3  $\mu_B$ /Mn saturation magnetization at 120 K with  $H=5$  T.

Anisotropic systems such as La<sub>1.2</sub>Sr<sub>1.8</sub>Mn<sub>2</sub>O<sub>7</sub> provide new opportunities to explore the connections between magnetic, electronic, and structural transitions in the CMR manganites. Like the perovskite-based CMR materials, the layered compound La<sub>1.2</sub>Sr<sub>1.8</sub>Mn<sub>2</sub>O<sub>7</sub> exhibits lattice effects correlated with ferromagnetic ordering and charge delocalization. Unlike its three-dimensional analogues, however, the Jahn-Teller distortion of the MnO<sub>6</sub> octahedra in this two-dimensional material increases as charge is delocalized. Such a result indicates that a model of the distortion relaxing upon electron delocalization may be an incomplete picture in low dimensional mixed-valent manganites. Indeed, our observation of a “one-long, five-short” geometry in the metallic phase indicates that a substantial distortion of a single Mn-O bond in the double layer of MnO<sub>6</sub> octahedra is not incompatible with an itinerant electron state. Indeed, the existence of a metallic state in such a distorted geometry underscores the need to better understand what geometric parameters control the competition between localized and itinerant electron states in the manganites as a whole. The behavior above  $T_C$ —a small ordered moment, a deviation from linearity in the in-plane thermal expansion—highlights the need for more detailed study of the connection between magnetism, transport, and structure in this particular class of CMR materials.

The authors thank P. G. Radaelli *et al.* for sharing their results on La<sub>0.35</sub>Pr<sub>0.35</sub>Ca<sub>0.3</sub>MnO<sub>3</sub>.<sup>13</sup> This work was supported by the U.S. Department of Energy, Basic Energy Sciences-Materials Sciences, and ER-LTT, under Contract No. W-31-109-ENG-38 (J.F.M., J.D.J., D.G.H., C.D.P., S.D.B.) and by the NSF Office of Science and Technology Centers under Grant No. DMR 91-20000 (D.N.A.).

<sup>1</sup>Y. Shimakawa, Y. Kubo, and T. Manako, *Nature* **379**, 53 (1996).

<sup>2</sup>S-W. Cheong, H. Y. Hwang, B. Batlogg, and L. W. Rupp, Jr., *Solid State Commun.* **98**, 163 (1996).

<sup>3</sup>Y. Moritomo, A. Asamitsu, H. Kuwahara, and Y. Tokura, *Nature* **380**, 141 (1996).

<sup>4</sup>J. D. Jorgensen, J. J. Faber, J. M. Carpenter, R. K. Crawford, J. R. Haumann, R. L. Hitterman, R. Kleb, G. E. Ostrowski, F. J. Rotella, and T. G. Worton, *J. Appl. Crystallogr.* **22**, 321 (1989).

<sup>5</sup>Y. Moritomo, Y. Tomioka, A. Asamitsu, Y. Tokura, and Y. Matsui, *Phys. Rev. B* **51**, 3297 (1995).

<sup>6</sup>R. A. Mohan Ram, P. Ganguly, and C. N. R. Rao, *J. Solid State Chem.* **70**, 82 (1987).

<sup>7</sup>R. Mahesh, R. Mahendiran, A. K. Raychaudhuri, and C. N. R. Rao, *J. Solid State Chem.* **122**, 448 (1996).

<sup>8</sup>J. B. MacChesney, J. F. Potter, and R. C. Sherwood, *J. Appl. Phys.* **40**, 1243 (1969).

<sup>9</sup>V. Caignaert, E. Suard, A. Maignan, C. Simon, and B. Raveau, *J. Magn. Magn. Mater.* **153**, L260 (1996).

<sup>10</sup>D. N. Argyriou, J. F. Mitchell, C. D. Potter, D. G. Hinks, J. D. Jorgensen, and S. D. Bader, *Phys. Rev. Lett.* **76**, 3826 (1996).

<sup>11</sup>M. R. Ibarra, P. A. Algarabel, C. Marquina, J. Biasco, and J. García, *Phys. Rev. Lett.* **75**, 3541 (1995).

<sup>12</sup>P. G. Radaelli, D. E. Cox, M. Marezio, S-W. Cheong, P. E. Schiffer, and A. P. Ramirez, *Phys. Rev. Lett.* **75**, 4488 (1995).

<sup>13</sup>P. G. Radaelli, M. Marezio, H. Y. Hwang, S-W. Cheong, and B. Batlogg (unpublished).

<sup>14</sup>W. Archibald, J.-S. Zhou, and J. B. Goodenough, *Phys. Rev. B* **53**, 14 445 (1996).

<sup>15</sup>J. B. Goodenough, *Prog. Solid State Chem.* **5**, 145 (1972).

<sup>16</sup>J. F. Mitchell, D. N. Argyriou, C. D. Potter, D. G. Hinks, J. D. Jorgensen, and S. D. Bader, *Phys. Rev. B* **54**, 6172 (1996).

<sup>17</sup>H. Y. Hwang, S-W. Cheong, P. G. Radaelli, M. Marezio, and B. Batlogg, *Phys. Rev. Lett.* **75**, 914 (1995).

<sup>18</sup>P. G. Radaelli, M. Marezio, H. Y. Hwang, and S-W. Cheong, *J. Solid State Chem.* **122**, 444 (1996).